a Brownian particle on a water surface with statistical mechanics. Some other systems, such as the earth's atmosphere, are in relatively fast motion, with limited thermal exchange. Such systems are described partly by statistical physics, but mostly by hydrodynamics, as is finally quite natural. We have seen in this subsection that hydrodynamics remains relevant to mechanical systems even in the long-time (equilibrium) limit, in the absence of thermal coupling to the outside world.

2.3 Pressure and the Boltzmann distribution

Equilibrium statistical mechanics contains two key concepts. The first and foremost is equiprobability, the principle that configurations with the same energy are equally probable. This is all we need for hard disks and spheres in a box of fixed volume. In this section, we address the second key concept, the Boltzmann distribution $\pi(a) \propto \mathrm{e}^{-\beta E(a)}$, which relates the probabilities $\pi(a)$ and $\pi(b)$ of configurations a and b with different energies. It comes up even for hard spheres if we allow variations in the box volume (see Fig. 2.31) and allow exchange of energy with an external bath. We thus consider a box at constant temperature and pressure rather than at constant temperature and volume.

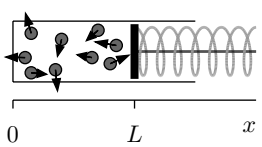

Fig. 2.31 A box with disks, closed off by a piston exerting a constant force.

For hard spheres, the constant-pressure ensemble allows density fluctuations on length scales larger than the fixed confines of the simulation box. The absence of such fluctuations is one of the major differences between a large and a periodic small system (see Fig. 2.32; the small system has exactly four disks per box, the large one between two and six). Our Monte Carlo algorithm for hard spheres at constant pressure is quite different from Alg. 2.7 (`direct-disks`), because it allows us to carry over some elements of a direct sampling algorithm for ideal particles. We shall discuss this non-interacting case first.

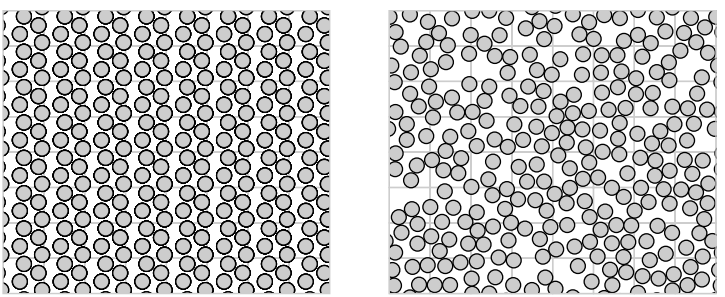

Fig. 2.32 256 disks at density $\eta = 0.48$. *Left*: periodically replicated system of four particles. *Right*: large periodic box.

2.3.1 Bath-and-plate system

To familiarize ourselves with the concept of pressure, we consider a box filled with hard disks and closed off by a piston, at position $x = L$. A spring pushes the piston to the left with constant force, independent of x (see Fig. 2.31). The particles and the piston have kinetic energy. The piston has also potential energy, which is stored in the spring. The sum of the two energies is constant. If the piston is far to the right, the particles have little kinetic energy, because potential energy is stored in the spring. In contrast, at small L, the particles are compressed and they have a higher kinetic energy. As the average kinetic energy is identified with the temperature (see Subsection 2.2.4), the disks are not only at variable volume but also at nonconstant temperature.

It is preferable to keep the piston–box system at constant temperature. We thus couple it to a large bath of disks through a loose elastic plate, which can move along the x-direction over a very small distance Δ (see Fig. 2.34). By zigzagging in this interval, the plate responds to hits from both the bath and the system. For concreteness, we suppose that the particles in the system and in the bath, and also the plate, all have a mass $m = 1$ (the spring itself is massless). All components are perfectly elastic. Head-on collisions between elastic particles of the same mass exchange the velocities (see Fig. 2.33), and the plate, once hit by a bath particle with an x-component of its velocity v_x will start vibrating with a velocity $\pm v_x$ inside its small interval (over the small distance Δ) until it eventually transfers this velocity to another particle, either in the box or in the bath.

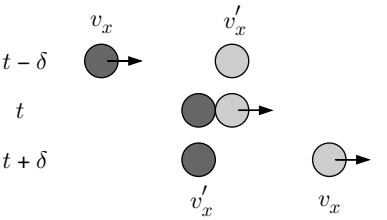

Fig. 2.33 Elastic head-on collision between equal-mass objects (case $v_x' = 0$ shown).

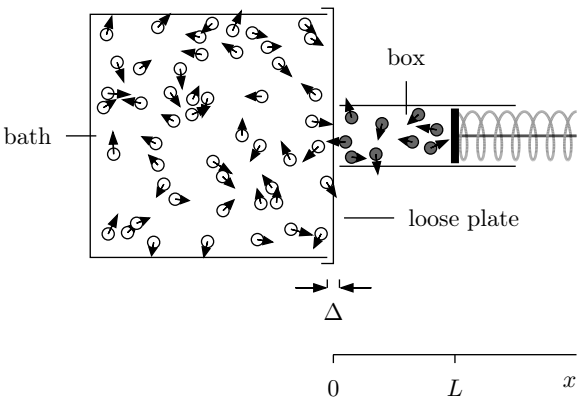

Fig. 2.34 The box containing particles shown in Fig. 2.31, coupled to an infinite bath through a loose plate.

The plate's velocity distribution—the fraction of time it spends at velocity v_x—is not the same as the Maxwell distribution of one velocity component for the particles. This is most easily seen for a bath of Maxwell-distributed noninteracting point particles (hard disks with zero

radius): fast particles zigzag more often between the plate and the left boundary of the bath than slow particles, biasing the distribution by a factor $|v_x|$:

$$\pi(v_x)\,\mathrm{d}v_x \propto |v_x| \exp\left(-\beta v_x^2/2\right) \mathrm{d}v_x. \tag{2.12}$$

We note that the Maxwell distribution for one velocity component lacks the $|v_x|$ term of eqn (2.12), and it is finite at $v_x = 0$. The biased distribution, however, must vanish at $v_x = 0$: to acquire zero velocity, the plate must be hit by a bath particle which itself has velocity zero (see Fig. 2.33). However, these particles do not move, and cannot get to the plate. This argument for a biased Maxwell distribution can be applied to a small layer of finite-size hard disks close to the plate, and eqn (2.12) remains valid.

The relatively infrequent collisions of the plate with box particles play no role in establishing the probability distribution of the plate velocity, and we may replace the bath and the plate exactly by a generator of biased Gaussian random velocities (with $v_x > 0$; see Fig. 2.33). The distribution in eqn (2.12) is formally equivalent to the Maxwell distribution for the absolute velocity in two dimensions, and so we can sample it with two independent Gaussians as follows:

$$\begin{aligned} &\{\Upsilon_1, \Upsilon_2\} \leftarrow \{\texttt{gauss}\,(1/\sqrt{\beta})\,, \texttt{gauss}\,(1/\sqrt{\beta})\}, \\ &v_x \leftarrow \sqrt{\Upsilon_1^2 + \Upsilon_2^2}. \end{aligned} \tag{2.13}$$

Alternatively, the sample transformation of Subsection 1.2.4 can also be applied to this problem:

$$\int_0^1 \mathrm{d}\Upsilon = c \int_0^\infty \mathrm{d}u\ \exp(-u) = c' \int_0^\infty \mathrm{d}v_x\ v_x \exp\left(-\beta v_x^2/2\right).$$

The leftmost integral is sampled by $\Upsilon = \texttt{ran}\,(0,1)$. The substitutions $\exp(-u) = \Upsilon$ and $\beta v_x^2/2 = u$ yield

$$v_x \leftarrow \sqrt{\frac{-2\log\left[\texttt{ran}\,(0,1)\right]}{\beta}}.$$

This routine is implemented in Alg. 2.10 (`maxwell-boundary`). It exactly replaces—integrates out—the infinite bath.

Maxwell boundary

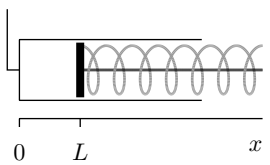

Fig. 2.35 A piston with Maxwell boundary conditions at $x = 0$.

procedure `maxwell-boundary`
input $\{v_x, v_y\}$ (disk in contact with plate)
$\Upsilon \leftarrow \texttt{ran}\,(0,1)$
$v_x \leftarrow \sqrt{-2\texttt{log}\,(\Upsilon)/\beta}$
output $\{v_x, v_y\}$

Algorithm 2.10 `maxwell-boundary`. Implementing Maxwell boundary conditions.

In conclusion, to study the box–bath–piston system, we need not set up a gigantic molecular dynamics simulation with particles on either

side of the loose plate. The bath can be integrated out exactly, to leave us with a pure box–piston model with Maxwell boundary conditions. These boundary conditions are of widespread use in real-life simulations, notably when the temperature varies through the system.

2.3.2 Piston-and-plate system

We continue our analysis of piston-and-plate systems, without a computer, for a piston in a box without disks, coupled to an infinite bath represented by Maxwell boundary conditions (see Fig. 2.35). The piston hits the plate $L = 0$ at times $\{\dots, t_i, t_{i+1}, \dots\}$. Between these times, it obeys Newton's equations with the *constant force* generated by the spring. The piston height satisfies $L(t - t_i) = v_0 \cdot (t - t_i) - \frac{1}{2}(t - t_i)^2$ (see Fig. 2.36). We take the piston mass and restoring force to be equal to one, and find

$$\underbrace{t_{i+1} - t_i}_{\substack{\text{time of flight} \\ \text{in Fig. 2.36}}} = 2v_0.$$

We see that the time the piston spends on a trajectory with initial velocity v_0 is proportional to v_0. We thus find the following:

$$\left\{ \begin{array}{c} \text{fraction of time spent} \\ \text{at initial velocities} \\ [v_0, v_0 + \mathrm{d}v_0] \end{array} \right\} \propto \overbrace{v_0}^{\text{time of flight}} \overbrace{v_0 \exp\left(-\beta v_0^2/2\right) \mathrm{d}v_0}^{\text{Maxwell boundary cond.}}.$$

During each flight, the energy is constant, and we can translate what we have found into a probability distribution of the energy E. Because $\mathrm{d}E = v_0\,\mathrm{d}v_0$, the time the piston spends in the interval of energies $[E, E+\mathrm{d}E]$—the probability $\pi(E)\,\mathrm{d}E$—is

$$\pi(E)\,\mathrm{d}E \propto \sqrt{E}\mathrm{e}^{-\beta E}\,\mathrm{d}E. \tag{2.14}$$

The factor $\sqrt{E}$ in eqn (2.14) is also obtained by considering the phase space of the moving piston, spanned by the variables L and v (see Fig. 2.37). States with an energy smaller than E are below the curve

$$L(E, v) = E - \frac{v^2}{2}.$$

The volume $\mathcal{V}(E)$ of phase space for energies $\leq E$ is given by

$$\mathcal{V}(E) = \int_0^{\sqrt{2E}} \mathrm{d}v \ \left[E - \frac{v^2}{2}\right] = \left[Ev - \frac{v^3}{6}\right]_0^{\sqrt{2E}} = \sqrt{2}\frac{2}{3}E^{3/2}.$$

It follows that the density of states for an energy E, that is, the number of phase space elements with energies between E and $E + \mathrm{d}E$, is given by

$$\mathcal{N}(E) = \frac{\partial}{\partial E}\mathcal{V}(E) = \sqrt{2E}.$$

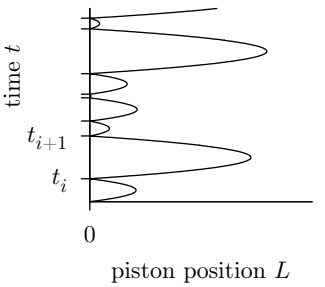

Fig. 2.36 Trajectory $\{L, t\}$ of a piston coupled to a plate with Maxwell boundary conditions at $L = 0$.

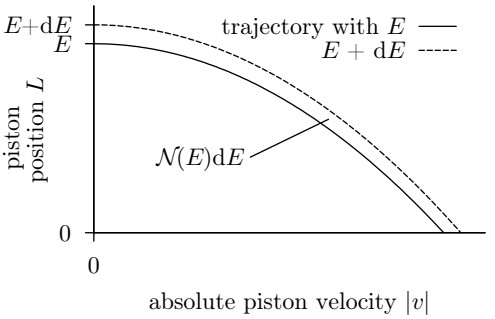

Fig. 2.37 Piston–plate system. The phase space for an energy in the interval $[E, E + \mathrm{d}E]$ has a volume $\mathcal{N}(E)\,\mathrm{d}E$.

So, we expect to have a probability $\pi(E)$ as follows:

$$\pi(E)\,\mathrm{d}E = \mathcal{N}(E)\,\mathrm{e}^{-\beta E}\,\mathrm{d}E.$$

It also follows that the system satisfies the equiprobability principle, that is, it spends equal amounts of time in the interval $\mathrm{d}x\ \mathrm{d}v$, whatever v is. This follows simply from the fact that $\mathrm{d}x$ is proportional to $\mathrm{d}E$ and $\mathrm{d}v$ is proportional to $\mathrm{d}t$:

$$\pi(x, v)\,\mathrm{d}x\,\mathrm{d}v = \exp\left[-\beta E(x, v)\right]\mathrm{d}x\,\mathrm{d}v.$$

This is the Boltzmann distribution, and we have derived it, as promised, from the equiprobability principle. We can also obtain the Boltzmann distribution for a piston–plate model with modified springs, for example with a potential energy $E(L) = L^\alpha$ with arbitrary positive α different from the case $\alpha = 1$ treated in this subsection (see Exerc. 2.15).

Our solution of the piston–plate model of Fig. 2.35 can be generalized to the case of a box containing particles in addition to the piston, the spring, and the vibrating plate. With more than one disk, we can no longer solve the equations of motion of the coupled system analytically, and have to suppose that for a fixed piston position and velocity of the piston all disk positions and velocities are equally probable, and also that for fixed disks, the parameters of the piston obey the Boltzmann distribution. The argument becomes quite involved. In the remainder of this book, we rather take for granted the two pillars of statistical physics, namely the equiprobability principle ($\pi(a) = \pi(E(a))$) and the Boltzmann distribution, and study their consequences, moving away from the foundations of statistical mechanics to what has been built on top of them.

2.3.3 Ideal gas at constant pressure

In this subsection, we work out some sampling methods for a one-dimensional gas of point particles interacting with a piston. What we learn here can be put to work for hard spheres and many other systems.

In this gas, particles at positions $\{x_1, \ldots, x_N\}$ on the positive axis may move about and pass through each other, but must satisfy $x_k < L$, where L is again the piston position, the one-dimensional volume of the box. The energy of the piston at position L is PL, where P is the pressure (see Fig. 2.38).

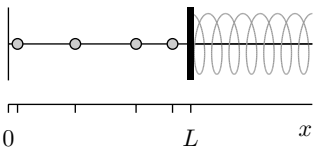

Fig. 2.38 Particles in a line, with a piston enforcing constant pressure, a restoring force independent of L.

The system composed of the N particles and the piston may be treated by Boltzmann statistical mechanics with a partition function

$$Z = \int_0^\infty \mathrm{d}L\ \mathrm{e}^{-\beta PL} \int_0^L \mathrm{d}x_1\ \ldots \int_0^L \mathrm{d}x_N, \tag{2.15}$$

which we can evaluate analytically:

$$Z = \int_0^\infty \mathrm{d}L\ \mathrm{e}^{-\beta PL} L^N = \frac{N!}{(\beta P)^{N+1}}.$$

We can use this to compute the mean volume $\langle L \rangle$ of our system,

$$\langle \text{Volume} \rangle = \langle L \rangle = \frac{\int_0^\infty \mathrm{d}L\ L^{N+1} \mathrm{e}^{-\beta PL}}{\int_0^\infty \mathrm{d}L\ L^N \mathrm{e}^{-\beta PL}} = \frac{N+1}{\beta P},$$

which gives essentially the ideal-gas law $PV = Nk_\mathrm{B}T$.

We may sample the integral in eqn (2.15) by a two-step approach. First, we fix L and directly sample particle positions to the left of the piston. Then, we fix the newly obtained particle positions $\{x_1, \ldots, x_N\}$ and sample a new piston position L, to the right of all particles, using the Metropolis algorithm (see Alg. 2.11 (`naive-piston-particles`) and Fig. 2.39). To make sure that it is correct to proceed in this way, we may write the partition function given in eqn (2.15) without L-dependent boundaries for the x-integration:

$$Z = \int_0^\infty \mathrm{d}L \int_0^\infty \mathrm{d}x_1\ \ldots \int_0^\infty \mathrm{d}x_N\ \mathrm{e}^{-\beta PL} \{L > \{x_1, \ldots, x_N\}\}. \tag{2.16}$$

The integrals over the positions $\{x_1, \ldots, x_N\}$ no longer have an L-dependent upper limit, and Alg. 2.11 (`naive-piston-particles`) is thus correct. The naive piston–particle algorithm can be improved: for fixed particle positions, the distribution of L, from eqn (2.16), is $\pi(L) \propto \mathrm{e}^{-\beta PL}$ for $L > x_\mathrm{max}$, so that $\Delta_L = L - x_\mathrm{max}$ can be sampled directly (see Alg. 2.12 (`naive-piston-particles(patch)`)). This Markov-chain algorithm consists of two interlocking direct-sampling algorithms which exchange the current values of x_max and L: one algorithm generates particle positions for a given L, and the other generates piston positions for given $\{x_1, \ldots, x_N\}$.

procedure `naive-piston-particles`
input L
$\{x_1, \ldots, x_N\} \leftarrow \{\texttt{ran}\,(0, L), \ldots, \texttt{ran}\,(0, L)\}$ (all indep.)
$x_{\max} \leftarrow \texttt{max}\,(x_1, \ldots, x_N)$
$\Delta_L \leftarrow \texttt{ran}\,(-\delta, \delta)$
$\Upsilon \leftarrow \exp(-\beta P \Delta_L)$
if ($\texttt{ran}\,(0,1) < \Upsilon$ and $L + \Delta_L > x_{\max}$) **then**
  $\{\ L \leftarrow L + \Delta_L$
output $L, \{x_1, \ldots, x_N\}$

Algorithm 2.11 `naive-piston-particles`. Markov-chain algorithm for one-dimensional point particles at pressure P (see patch in Alg. 2.12).

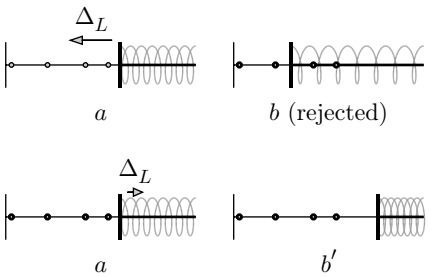

Fig. 2.39 Piston moves in Alg. 2.11 (`naive-piston-particles`). The move $a \to b'$ is accepted with probability $\exp(-\beta P \Delta_L)$.

We can construct a direct-sampling algorithm by a simple change of variables in the partition function Z:

$$Z = \int_0^\infty \mathrm{d}L\ L^N \int_0^L \frac{\mathrm{d}x_1}{L}\ \ldots \int_0^L \frac{\mathrm{d}x_N}{L}\ \mathrm{e}^{-\beta P L} \tag{2.17}$$

$$= \underbrace{\int_0^\infty \mathrm{d}L\ L^N \mathrm{e}^{-\beta P L}}_{\substack{\text{sample from} \\ \text{gamma distribution}}} \underbrace{\int_0^1 \mathrm{d}\alpha_1\ \ldots \int_0^1 \mathrm{d}\alpha_N}_{\substack{\text{sample as } \alpha_k = \texttt{ran}\,(0,1) \\ \text{for } k = 1, \ldots, N}} . \tag{2.18}$$

The integration limits for the variables $\{\alpha_1, \ldots, \alpha_N\}$ no longer depend on L, and the piston and particles are decoupled. The first integral in eqn (2.18) is a rescaled gamma distribution $\pi(x) \propto x^N \mathrm{e}^{-x}$ with $x = \beta P L$ (see Fig. 2.40), and gamma-distributed random numbers can be directly sampled as a sum of $N + 1$ exponential random numbers. For $N = 0$, $\pi(x)$ is a single exponential random variable. For $N = 1$, it is sampled by the sum of two independent exponential random numbers, whose

procedure `naive-piston-particles(patch)`
input L
$\{x_1, \ldots, x_N\} \leftarrow \{\texttt{ran}\,(0, L), \ldots, \texttt{ran}\,(0, L)\}$
$x_{\max} \leftarrow \texttt{max}\,(x_1, \ldots, x_N)$
$\Delta_L \leftarrow -\texttt{log}\,(\texttt{ran}\,(0, 1))\,/(\beta P)$
$L \leftarrow x_{\max} + \Delta_L$
output $L, \{x_1, \ldots, x_N\}$

Algorithm 2.12 `naive-piston-particles(patch)`. Implementing direct sampling of L into the Markov-chain algorithm for $\{x_1, \ldots, x_N\}$.

distribution, the convolution of the original distributions, is given by

$$\begin{aligned}\pi(x) &= \int_0^x \mathrm{d}y\ \mathrm{e}^{-y}\mathrm{e}^{-(x-y)} \\ &= \mathrm{e}^{-x}\int_0^x \mathrm{d}y\ = x\mathrm{e}^{-x}\end{aligned}$$

(see Subsection 1.3.1). More generally, a gamma-distributed random variable taking values x with probability $\Gamma_N(x)$ can be sampled by the sum of logarithms of $N+1$ random numbers, or, better, by the logarithm of the product of the random numbers, to be computed alongside the α_k. It remains to rescale the gamma-distributed sample x into the size of the box, and the random numbers $\{\alpha_1, \ldots, \alpha_N\}$ into particle positions (see Alg. 2.13 (`direct-piston-particles`)).

procedure `direct-piston-particles`
$\Upsilon \leftarrow \texttt{ran}\,(0, 1)$
for $k = 1, \ldots, N$ **do**
$\left\{\begin{array}{l}\alpha_k \leftarrow \texttt{ran}\,(0, 1)\\ \Upsilon \leftarrow \Upsilon\texttt{ran}\,(0, 1)\end{array}\right.$
$L \leftarrow -\texttt{log}\,(\Upsilon)\,/(\beta P)$
output $L, \{\alpha_1 L, \ldots, \alpha_N L\}$

Algorithm 2.13 `direct-piston-particles`. Direct sampling of one-dimensional point particles and a piston at pressure P.

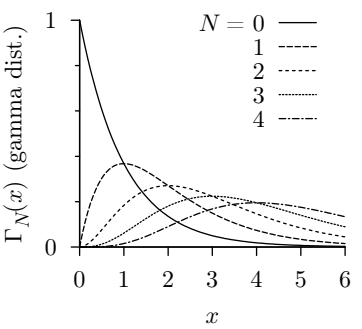

Fig. 2.40 Gamma distribution $\Gamma_N(x) = x^N\mathrm{e}^{-x}/N!$, the distribution of the sum of $N + 1$ exponentially distributed random numbers.

2.3.4 Constant-pressure simulation of hard spheres

It takes only a few moments to adapt the direct-sampling algorithm for one-dimensional particles to hard spheres in a d-dimensional box of variable volume V (and fixed aspect ratio) with $\pi(V) \propto \exp(-\beta PV)$. We simply replace the piston by a rescaling of the box volume and take into account the fact that the sides of the box scale with the dth root of the volume. We then check whether the output is a legal hard-sphere configuration (see Alg. 2.14 (`direct-p-disks`)). This direct-sampling algorithm mirrors Alg. 2.7 (`direct-disks`) (see Fig. 2.41).

procedure `direct-p-disks`
1 $\Upsilon \leftarrow \texttt{ran}\,(0,1)$
for $k = 1, \ldots, N$ **do**
$\left\{ \begin{array}{l} \boldsymbol{\alpha}_k \leftarrow \{\texttt{ran}\,(0,1), \texttt{ran}\,(0,1)\} \\ \Upsilon \leftarrow \Upsilon\texttt{ran}\,(0,1) \end{array} \right.$
$L \leftarrow \sqrt{-\texttt{log}\,(\Upsilon)/(\beta P)}$
for $k = 1, \ldots, N$ **do**
$\{ \ \mathbf{x}_k \leftarrow L\boldsymbol{\alpha}_k$
if $(\{\{\mathbf{x}_1, \ldots, \mathbf{x}_N\}, L\}$ not a legal configuration**) goto** 1
output $L, \{\mathbf{x}_1, \ldots, \mathbf{x}_N\}$

Algorithm 2.14 `direct-p-disks`. Direct sampling for N disks in a square box with periodic boundary conditions at pressure P.

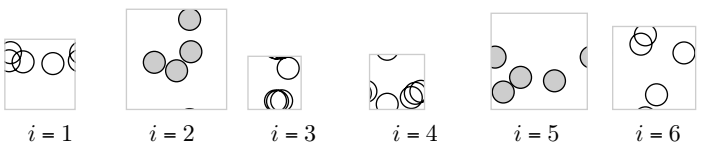

Fig. 2.41 Direct sampling for four hard disks at constant pressure (from Alg. 2.14 (`direct-p-disks`)).

We again have to migrate to a Markov-chain Monte Carlo algorithm, allowing for changes in the volume and for changes in the particle positions, the variables $\{\boldsymbol{\alpha}_1, \ldots, \boldsymbol{\alpha}_N\}$. Although we cannot hope for a rejection-free direct-sampling algorithm for hard spheres, we shall see that the particle rescaling and the direct sampling of the volume carry over to this interacting system.

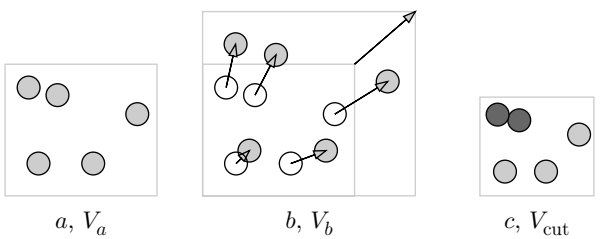

Fig. 2.42 Disk configurations with fixed $\{\boldsymbol{\alpha}_1, \ldots, \boldsymbol{\alpha}_N\}$. Configuration c is at the lower cutoff volume.

Let us consider a fixed configuration $\boldsymbol{\alpha} = \{\boldsymbol{\alpha}_1, \ldots, \boldsymbol{\alpha}_N\}$. It can exist at any box dimension which is sufficiently big to make it into a legal hard-sphere configuration. What happens for different volumes at fixed $\boldsymbol{\alpha}$ is shown in Fig. 2.42: the particle positions are blown up together with the

box, but the radii of the disks remain the same. There is an α-dependent lower cutoff (minimum) volume, $V_{\rm cut}$, below which configurations are rejected.

Above $V_{\rm cut}$, the rescaled volume $x = \beta PV$ (with $x_{\rm cut} = \beta PV_{\rm cut}$) is distributed with what is called the gamma-cut distribution:

$$\pi(x) = \Gamma_N^{\rm cut}(x, x_{\rm cut}) \propto \begin{cases} x^N \mathrm{e}^{-x} & \text{for } x > x_{\rm cut} \\ 0 & \text{otherwise} \end{cases} .$$

As always in one dimension, the gamma-cut distribution can be directly sampled. We can compare it above $x_{\rm cut} > N$ with an exponential:

$$\begin{aligned} \underline{\Gamma_N^{\rm cut}(x, x_{\rm cut})} \propto \pi_\Gamma(x, x_{\rm cut}) &= \left(\frac{x}{x_{\rm cut}}\right)^N \exp\left[-(x - x_{\rm cut})\right] \\ &= \exp\left[-(x - x_{\rm cut}) + N \log \frac{x}{x_{\rm cut}}\right] \\ &= \exp\Bigg[-(x - x_{\rm cut}) + N \underbrace{\log\left(1 + \frac{x - x_{\rm cut}}{x_{\rm cut}}\right)}_{< (x - x_{\rm cut})/x_{\rm cut}}\Bigg] \\ &< \overbrace{\underline{\exp\left[-(1 - N/x_{\rm cut})(x - x_{\rm cut})\right]}}^{\pi_{\rm exp}(x, x_{\rm cut})} . \end{aligned} \tag{2.19}$$

To sample the gamma-cut distribution, we adapt the rejection method of Subsection 1.2.4, and rather sample the exponential distribution, which is everywhere larger. We thus throw uniformly distributed pebbles into the region delimited by $x \in [x_{\rm cut}, \infty]$ and $y \in [0, \pi_{\rm exp}(x)]$ (see Fig. 2.43). x can be sampled from $\pi_{\rm exp}(x, x_{\rm cut})$, and y can be sampled as a random number between 0 and $\pi_{\rm exp}(x)$. We must reject the pebble if $y = \texttt{ran}\,(0, \pi_{\rm exp}(x))$ is above the gamma-cut distribution, in other words if $y = \pi_{\rm exp}(x)\texttt{ran}\,(0, 1) > \pi_\Gamma(x)$ (see Alg. 2.15 (`gamma-cut`)).

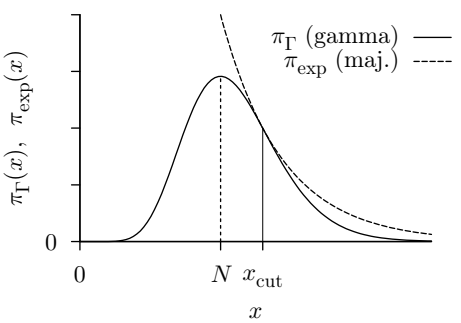

Fig. 2.43 Gamma distribution $\Gamma_N(x) \propto \pi_\Gamma = x^N \mathrm{e}^{-x}$, and its exponential majoration $\pi_{\rm exp}$, which allows us to sample the gamma-cut distribution.

procedure `gamma-cut`
input $x_{\rm cut}$
$x^* \leftarrow 1 - N/x_{\rm cut}$
if $(x^* < 0)$ **exit**
1 $\Delta_x \leftarrow -\texttt{log}\,(\texttt{ran}\,(0,1))\,/x^*$
$x \leftarrow x_{\rm cut} + \Delta_x$
$\Upsilon' \leftarrow (x/x_{\rm cut})^N \exp\left[-(1-x^*)\Delta_x\right]$
if $(\texttt{ran}\,(0,1) > \Upsilon')$ **goto** 1 (reject sample)
output $x_{\rm cut} + \Delta_x$

Algorithm 2.15 `gamma-cut`. Sampling the Gamma distribution for $x > x_{\rm cut} > N$.

Alg. 2.15 (`gamma-cut`) rapidly samples the gamma-cut distribution for any N and, after rescaling, a legal box volume for a fixed configuration $\boldsymbol{\alpha}$ (see Alg. 2.16 (`rescale-volume`)). The algorithm is due to Wood (1968). It must be sandwiched in between runs of constant-volume Monte Carlo calculations, and provides a powerful hard-sphere algorithm in the NPT ensemble, with the particle number, the pressure, and the temperature all kept constant.

procedure `rescale-volume`
input $\{L_x, L_y\}, \{\mathbf{x}_1, \ldots, \mathbf{x}_N\}$
$V \leftarrow L_x L_y$
$\sigma_{\rm cut} \leftarrow \min_{k,l}\left[\texttt{dist}\,(\mathbf{x}_k, \mathbf{x}_l)\right]$
$x_{\rm cut} \leftarrow \beta P V \cdot (\sigma/\sigma_{\rm cut})^2$
$V_{\rm new} \leftarrow \left[\texttt{gamma-cut}(N, x_{\rm cut})\right]/(\beta P)$
$\Upsilon \leftarrow \sqrt{V_{\rm new}/V}$
output $\{\Upsilon L_x, \Upsilon L_y\}, \{\Upsilon \mathbf{x}_1, \ldots, \Upsilon \mathbf{x}_N\}$

Algorithm 2.16 `rescale-volume`. Sampling and rescaling the box dimensions and particle coordinates for hard disks at constant P.

Finally, we note that, for hard spheres, the pressure P and inverse temperature $\beta = 1/(k_{\rm B}T)$ always appear as a product βP in the Boltzmann factor $\mathrm{e}^{-\beta PV}$. For hard spheres at constant volume, the pressure is thus proportional to the temperature, as was clearly spelled out by Daniel Bernoulli in the first scientific work on hard spheres, in 1733, long before the advent of the kinetic theory of gases and the statistical interpretation of the temperature. Bernoulli noticed, so to speak, that if a molecular dynamics simulation is run at twice the original speed, the particles will hit the walls twice as hard and transfer a double amount of the original momentum to the wall. But this transfer takes place in half the original time, so that the pressure must be four times larger. This implies that the pressure is proportional to $v^2 \propto T$.